World Journal of Clinical Oncology

Submit a Manuscript: https://www.f6publishing.com

World J Clin Oncol 2024 January 24; 15(1): 115-129

DOI: 10.5306/wjco.v15.i1.115

ISSN 2218-4333 (online)

ORIGINAL ARTICLE

Clinical and Translational Research

Gene signatures to therapeutics: Assessing the potential of ivermectin against t(4;14) multiple myeloma

Yang Song, Hao-Jun Zhang, Xia Song, Jie Geng, Hong-Yi Li, Li-Zhong Zhang, Bo Yang, Xue-Chun Lu

Specialty type: Oncology

Provenance and peer review: Unsolicited article; Externally peer reviewed.

Peer-review model: Single blind

Peer-review report's scientific quality classification

Grade A (Excellent): 0
Grade B (Very good): B
Grade C (Good): 0
Grade D (Fair): 0
Grade E (Poor): 0

P-Reviewer: Blanc R, France

Received: November 20, 2023
Peer-review started: November 20, 2023
First decision: December 5, 2023
Revised: December 13, 2023
Accepted: January 2, 2024
Article in press: January 2, 2024
Published online: January 24, 2024

Yang Song, Hong-Yi Li, School of Basic Medicine, Medical School of Chinese PLA, Beijing 100853, China

Hao-Jun Zhang, Xia Song, Jie Geng, Li-Zhong Zhang, School of Basic Medicine, Shanxi Medical University, Taiyuan 030001, Shanxi Province, China

Bo Yang, Xue-Chun Lu, Department of Hematology, The Second Medical Centre, Chinese PLA General Hospital, Beijing 100853, China

Corresponding author: Xue-Chun Lu, PhD, Chief Doctor, Professor, Research Scientist, Department of Hematology, The Second Medical Center, Chinese PLA General Hospital, No. 28 Fuxing Road, Haidian District, Beijing 100853, China. luxuechun@301hospital.com.cn

Abstract

BACKGROUND

Multiple myeloma (MM) is a terminal differentiated B-cell tumor disease characterized by clonal proliferation of malignant plasma cells and excessive levels of monoclonal immunoglobulins in the bone marrow. The translocation, (t)(4;14), results in high-risk MM with limited treatment alternatives. Thus, there is an urgent need for identification and validation of potential treatments for this MM subtype. Microarray data and sequencing information from public databases could offer opportunities for the discovery of new diagnostic or therapeutic targets.

AIM

To elucidate the molecular basis and search for potential effective drugs of t(4;14) MM subtype by employing a comprehensive approach.

METHODS

The transcriptional signature of t(4;14) MM was sourced from the Gene Expression Omnibus. Two datasets, GSE16558 and GSE116294, which included 17 and 15 t(4;14) MM bone marrow samples, and five and four normal bone marrow samples, respectively. After the differentially expressed genes were identified, the Cytohubba tool was used to screen for hub genes. Then, the hub genes were analyzed using Gene Ontology and Kyoto Encyclopedia of Genes and Genomes analysis. Using the STRING database and Cytoscape, protein–protein interaction networks and core targets were identified. Potential small-molecule drugs were identified and validated using the Connectivity Map database and molecular

docking analysis, respectively.

RESULTS

In this study, a total of 258 differentially expressed genes with enriched functions in cancer pathways, namely cytokine receptor interactions, nuclear factor (NF)-κB signaling pathway, lipid metabolism, atherosclerosis, and Hippo signaling pathway, were identified. Ten hub genes (*cd45, vcam1, ccl3, cd56, app, cd48, btk, ccr2, cybb,* and *cxcl12*) were identified. Nine drugs, including ivermectin, deforolimus, and isoliquiritigenin, were predicted by the Connectivity Map database to have potential therapeutic effects on t (4;14) MM. In molecular docking, ivermectin showed strong binding affinity to all 10 identified targets, especially *cd45* and *cybb*. Ivermectin inhibited t(4;14) MM cell growth *via* the NF-κB pathway and induced MM cell apoptosis in vitro. Furthermore, ivermectin increased reactive oxygen species accumulation and altered the mitochondrial membrane potential in t(4;14) MM cells.

CONCLUSION

Collectively, the findings offer valuable molecular insights for biomarker validation and potential drug development in t(4;14) MM diagnosis and treatment, with ivermectin emerging as a potential therapeutic alternative.

Key Words: Multiple myeloma; Functional enrichment analysis; Molecular docking simulation; Gene expression profiling; Therapeutic target; Ivermectin

Core Tip: Multiple myeloma is a hematological malignancy with a significant impact on public health, and the t(4;14) subtype is particularly aggressive and resistant to existing treatments. Our study addresses the urgent need for new therapeutic approaches by employing a comprehensive approach that includes bioinformatics analysis, molecular docking, and experimental validation. We identified ten key genes associated with t(4;14) multiple myeloma (MM), shedding light on the molecular basis of this subtype. We explored the potential of ivermectin to assess whether it may be "repurposed" as a therapeutic agent for t(4;14) MM. Our findings indicate that ivermectin not only inhibits MM cell growth but also induces apoptosis *via* the nuclear factor-κB signaling pathway.

Citation: Song Y, Zhang HJ, Song X, Geng J, Li HY, Zhang LZ, Yang B, Lu XC. Gene signatures to therapeutics: Assessing the potential of ivermectin against t(4;14) multiple myeloma. *World J Clin Oncol* 2024; 15(1): 115-129
URL: https://www.wjgnet.com/2218-4333/full/v15/i1/115.htm
DOI: https://dx.doi.org/10.5306/wjco.v15.i1.115

INTRODUCTION

Multiple myeloma (MM) represents a severe hematological malignancy, affecting 176404 individuals and resulting in117077 fatalities annually[1]. MM is characterized by uncontrolled plasma cell proliferation in the bone marrow, leading to severe complications, such as bone and kidney damage, anemia, and hypercalcemia[2]. Of particular concern is the t(4;14) subtype, comprising up to 15% of new MM cases, with notably low survival rates and strong resistance to existing therapies[3]. Thus, effectively addressing this subtype remains an important medical challenge. Although the seminal research of Foltz *et al*[4] and Ashby *et al*[5] have provided insights into the pivotal facets of t(4;14) MM (Supplementary Table 1),which have advanced our understanding of this malignancy, certain aspects remain elusive.

Translational medicine is increasingly considering drug repurposing as a potential strategy to develop efficient, safe, cost-effective, and readily available anticancer treatments[6]. Advances in high-throughput sequencing technology have expanded biomedical and computational resources, facilitating a deeper understanding of cancer etiology and drug-target interactions, thus enabling drug repurposing[7]. Notably, the Connectivity Map (CMap) tool, housing a comprehensive dataset of 7000 microarrays from various cancer cells treated with 1309 molecular compounds, has been instrumental in identifying potential treatments for various cancers[8]. Notably, Shi *et al*[9] used CMap to identify eugenol as a potential treatment for triple-negative breast cancer, and Qiu *et al*[10] computationally identified small-molecule drugs with the potential to treat cervical cancer.

There is an urgent need for identification and validation of potential treatments for this MM subtype, therefore, we aim to elucidate the molecular basis and search for potential effective drugs by employing a comprehensive approach. We hope to contribute to advancing early MM diagnosis and tailoring its treatment.

MATERIALS AND METHODS

Differential expression analysis

The Gene Expression Omnibus (GEO) database (https://www.ncbi.nlm.nih.gov/gds) is a key public repository housing high-throughput gene expression data, microarray data, and gene chip information. For this study, we sourced the t(4;14) MM-related expression dataset from GEO. Our search parameters were tailored to t(4;14) MM across all fields, combined with filters for "Homo sapiens" as the organism and "dataset." Two datasets, GSE16558 and GSE116294, which included 17 and 15 t(4;14) MM bone marrow samples, and five and four normal bone marrow samples, respectively (Supplementary Table 2), were further considered for our analysis. To identify DEGs between the t(4;14) MM samples and normal samples, we used the "limma" package in R software [version 4.2.2, (http://www.R-project.org/)]. Our selection criteria were a P value < 0.05 and absolute log2 fold change (FC) > 1.

PPI network analysis

To construct a functional PPI network for the identified DEGs, we used the STRING online database tool (https://string-db.org/)[11]. Our selected threshold required a credibility score of > 0.4 for inclusion within the network. The Cytoscape software [version 3.10.1, (https://cytoscape.org/)] was used to visually map the PPI, offering a clear understanding of protein interactions.

Hub gene mapping

Using Cytoscape, the molecular complex detection (MCODE) plugin was activated to highlight prominent clusters, abiding by criteria, such as an MCODE score > 6 and a node count > 4. The CytoHubba plugin[12] within Cytoscape, paired with the Maximal Clique Centrality (MCC) method, was used to filter and identify the top-ranking genes. A combination of results drawn from the MCODE, MCC, and degree scores led to the identification of 10 key hub genes.

Functional enrichment analysis

The enrichment analysis was performed using the "GSEApy" package within Python (v.3.11.4, [https://www.python.org]), using the Kyoto Encyclopedia of Genes and Genomes (KEGG) and Gene Ontology. Subsequently, statistical significance was evaluated using the p-value, whereas the visualization of data was achieved using the "ggplot2" package in R. Gene Set Enrichment Analysis (GSEA) was performed using its dedicated software, sourcing gene sets from the Molecular Signature Database (http://software.broadinstitute.org/gsea/index.jsp).

Drug screening using CMap

The CMap database (https://clue.io)[13], a key tool in systems biology, was used to identify potential therapeutic candidates. Our criteria were rigorous, with a cutoff score of < −80.

Molecular docking

For our molecular docking investigations, 3D structural models of the proteins encoded by target genes were retrieved from UniProt[14] and Protein Data Bank databases and augmented with AlphaFold data. Focusing on structures determined *via* X-ray diffraction with a co-crystal resolution < 2.5 Å, we downloaded the 2D structural model of ivermectin from PubChem[15] and converted it into a 3D structure using the LigPrep module in Maestro. AutoDockTools were used to preprocess the ligands. Optimization included water removal, hydrogenation, charge determination, and torsion centers and bond selection, yielding a pdbqt file suitable for docking studies. Macromolecular docking calculations were performed using Vina software [version 1.1.2, (http://vina.scripps.edu/)]. To illustrate the post-docking ligand-receptor interactions, we used Ligplot+[16] for 2D mapping and PyMOL[17] for in-depth 3D analysis.

Reagents and antibodies

Ivermectin was purchased from Aladdin Biological Technology (Shanghai, China). The following primary antibodies were purchased from CST (Danvers, MA, United States): Anti- poly (ADP-ribose) polymerase (PARP) (9532; 1:1000), anti-cleaved PARP (5625; 1:1000), anti-cleaved caspase 3 (9661; 1:500), anti-cleaved caspase 9 (20750; 1:1000), and β-actin (3700; 1:1000). The following primary antibodies were purchased from Abcam (Cambridge, United Kingdom): Anti-B-cell lymphoma 2 (Bcl2; ab182858; 1:1000), anti-Bcl-2-associated X protein (Bax; ab32503; 1:1000), anti-NF-κB p65 (ab32536; 1:1000), anti-NF-κB p65 (phospho S536) (ab86299; 1:1000), anti-inhibitor of NF-κB (IκB) alpha (ab32518; 1:1000), and anti-IκB alpha (phospho-S36) (ab133462; 1:1000). The following secondary antibodies were purchased from Beyotime Biotechnology (Shanghai, China): anti-rabbit IgG (A0208; 1:5000) and anti-mouse IgG (A0216; 1:5000).

Cell culture

NCI-H929, a t(4;14) MM cell line, was obtained from the Cell Bank of the Type Culture Collection of the Chinese Academy of Sciences (Shanghai, China). The cells were cultured in RPMI-1640 medium (Gibco, Billings, MO, United States) with 10% fetal bovine serum (Gibco) and 1% penicillin/streptomycin (Gibco) at 37 °C with 5% CO_2. Preliminary tests confirmed that the cell lines were *Mycoplasma*-free.

Cytotoxic activity assay

To assess cytotoxic activity, 5000 cells were seeded per well into a 96-well plate and exposed to ivermectin concentrations ranging from 0–20 μmol/L for 24–48 h. After incubation, cell viability was evaluated using Cell Counting Kit-8 (CCK8)

(DojinDo, Shanghai, China), which required an additional 2-h incubation with 10 μL of CCK8 solution at 37 °C. The absorbance of the reaction mixture was measured at 450 nm using a microplate reader (Thermo Fisher Scientific, California, United States). The inhibitory concentration 50% (IC_{50}) of ivermectin for each cell type was determined from the viability data using GraphPad Prism v.10 and the following equation:

[(As−Ab)/(Ac−Ab)] × 100%, where "As," "Ac," and "Ab" are the absorbance values in the experimental, control, and blank wells, respectively.

Apoptosis assay

Cells were seeded into 6-well plates and treated with ivermectin for 24 h. After treatment, the cells were collected by centrifugation. They were then stained using the fluorescein isothiocyanate (FITC) Annexin V Apoptosis Detection Kit with 7-aminoactinomycin D (7-AAD; 640922; BioLegend, San Diego, CA, United States) by adding 5 μL of FITC conjugated with annexin V and 5 μL of 7-AAD solution. This was followed by 15 min incubation in the dark at 25 °C. Subsequently, the stained cells were analyzed using a flow cytometer (LSRFortessa; BD, Franklin Lakes, NJ, United States), and the data obtained were processed and interpreted using FlowJo software (v.10.4).

Reactive oxygen species assay

The cells were cultured in 6-well plates overnight. Fresh RPMI-1640 medium containing the indicated concentrations of ivermectin was added, and the cells were cultured for 24 h. A reactive oxygen species (ROS) assay kit (S0033S; Beyotime) was used to detect intracellular ROS levels using the following protocol: treated cells were incubated with 2′,7′-dichlorodihydrofluorescein diacetate for 20 min at 37 °C. Cells were washed thrice with serum-free medium, and images were acquired using a fluorescent inverted microscope (Olympus, Tokyo, Japan).

Mitochondrial membrane potential assay

Cells were first allowed to settle in 6-well plates, after which they were treated with ivermectin for 24 h. A JC-1 assay kit (M34152; Thermo Fisher Scientific) was used to evaluate the mitochondrial membrane potential within these cells. The assessment was performed in strict accordance with the manufacturer's guidelines. Readings from this assessment were captured using a flow cytometer (LSRFortessa; BD).

Western blot analysis

After 48 h of ivermectin treatment, the cells were harvested and lysed using Cell Lysis Buffer (P0013; Beyotime), which included a protease inhibitor. The subsequent lysate was subjected to a 30-min ice bath before centrifugation at 12000 rpm for 20 min at 4 °C. Proteins were quantified using a BCA assay kit (P0010; Beyotime), separated by sodium dodecyl-sulfate polyacrylamide gel electrophoresis, and transferred onto polyvinylidene fluoride membranes. Subsequently, these membranes were blocked with 5% skim milk for 2 h and incubated with primary antibodies overnight at 4 °C. After thorough washing, the membranes were incubated with horseradish peroxidase-conjugated secondary antibodies for 1 h at 25 °C. The proteins were visualized using an electrochemiluminescence kit (NCM Biotech, Suzhou, China).

Statistical analysis

All statistical evaluations were performed using both the R package and GraphPad Prism v.9.0 (GraphPad Software Inc., San Diego, CA, United States). Student's *t*-test was used to compare the means between two groups. Comparisons across multiple groups were conducted using one- and two-way ANOVA. All results are presented as the mean ± SD. Statistical significance was set at P levels < 0.05.

RESULTS

Identification of DEGs

We identified 1,100 DEGs (270 upregulated and 830 downregulated) and 1746 DEGs (808 upregulated and 938 downregulated) in the GSE16558 and GSE116294 datasets, respectively. These microarray findings have been presented using heat maps and volcano graphs, applying a threshold of P < 0.05, logFC<1 for downregulated genes, and logFC>1 for upregulated genes (Supplementary Figure 1).

Potential targets involved in t(4;14) MM and PPI network: To better understand the therapeutic pathways involved in t(4;14) MM, we constructed a Venn diagram and identified 258 probable targets related to t(4;14) MM (Figure 1A). Subsequently, a PPI network containing these targets was constructed to elucidate the target interrelations. The PPI network comprised 175 nodes and 697 edges (Figure 1B). Three targets that lacked interactions with other targets were excluded from the assessment. The top five identified nodes were cd45, btk, ccl3, cdh1, and cxcl12, highlighting their pivotal roles in the network.

Identification of clusters and hub targets in the PPI network

Using the Cytoscape MCODE plugin, we identified two clusters with scores > 6 (Figure 1C). The first group, with 57 nodes and 343 edges, was centered on the seed gene, *CD45*, and was predominantly related to altered transcriptional regulation in cancer. The second smaller cluster, which included 15 nodes and 66 edges, had *TLR1* as its seed gene and was primarily related to the negative regulation of apoptosis and signal transduction. Subsequently, the CytoHubba score

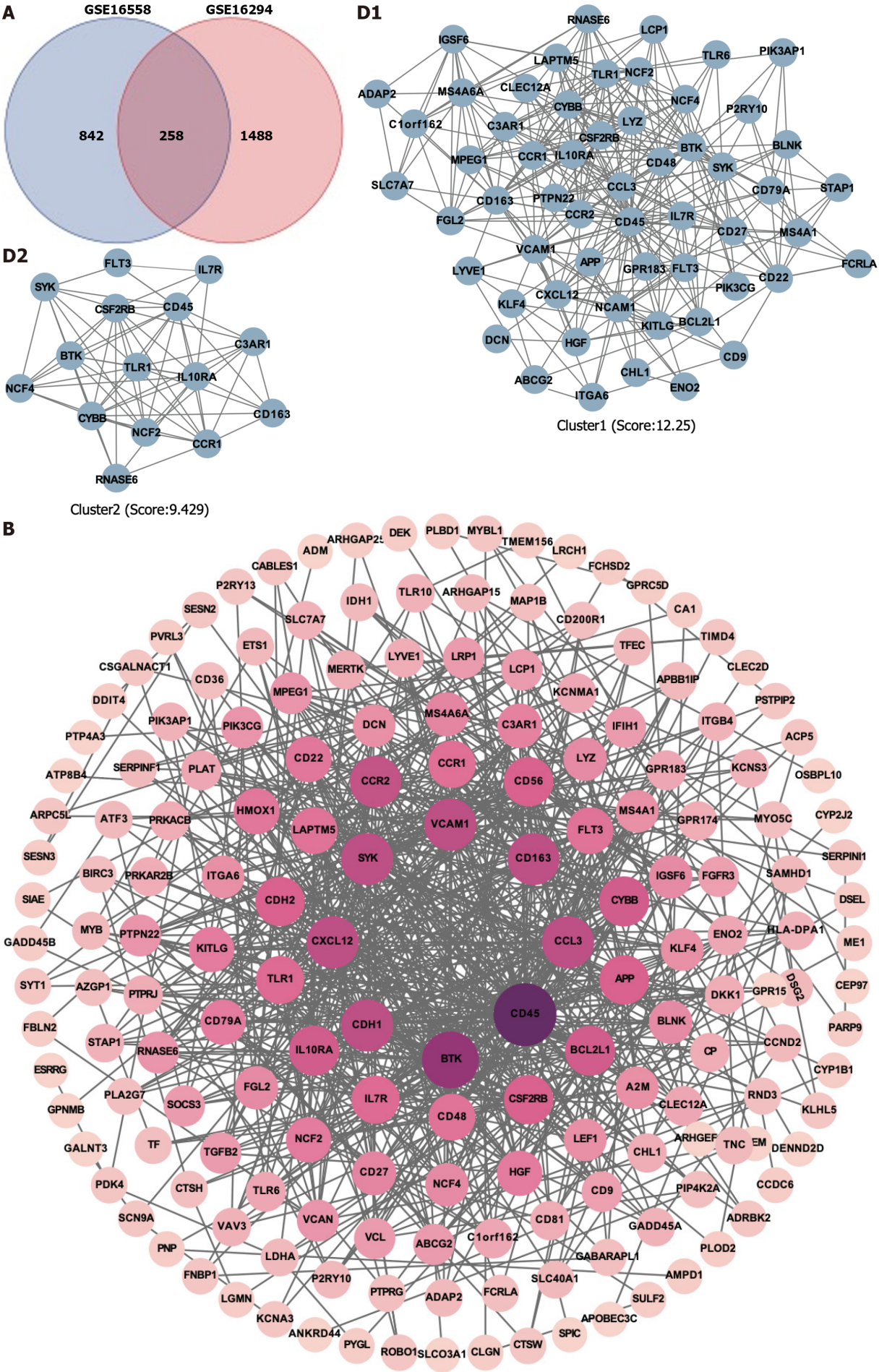
A
GSE16558
GSE16294
842
258
1488
D1
Cluster1 (Score:12.25)
D2
Cluster2 (Score:9.429)
B

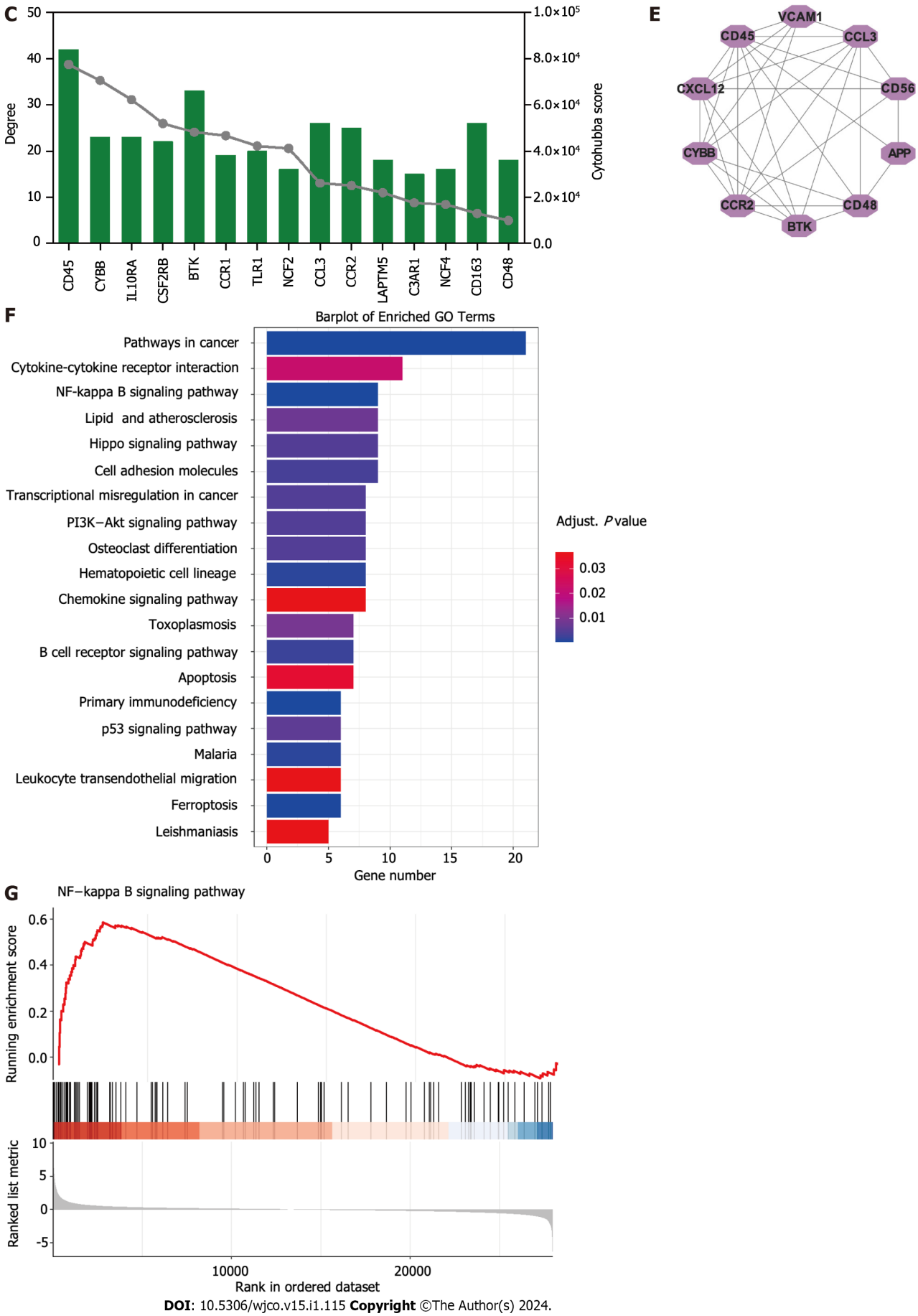

DOI: 10.5306/wjco.v15.i1.115

Figure 1 Identification of hub targets and the Kyoto Encyclopedia of Genes and Genomes pathways. A: Venn diagram illustrating overlap of

targets between GSE16558 and GSE116294 datasets; B: Target protein–protein interaction (PPI) network; C: Top 15 hub genes identified using CytoHubba plugin; D: Two primary clusters of PPI scored using themolecular complex detection plugin; E: Ranking of top 10 hub genes within PPI network; F: The Kyoto Encyclopedia of Genes and Genomes pathway enrichment analysis; G: Gene Set Enrichment Analysis of nuclear factor -κB signaling pathway. NK: Nuclear factor.

was used to identify the top 15 genes (Figure 1D). Each of these 15 genes had a degree score >15, indicating comprehensive interactions among them. Combining insights from MCODE, MCC, and degree scores, we identified 10 central hub genes: *cd45*, *vcam1*, *ccl3*, *cd56*, *app*, *cd48*, *btk*, *ccr2*, *cybb*, and *cxcl12* (Figure 1E).

Functional enrichment analysis

To better understand the potential therapeutic targets of t(4;14) MM, we performed functional enrichment analysis of the 255 shared targets. Using the KEGG database, we identified 232 enriched signal pathway terms through enrichment analysis. With an adjusted *P* value of < 0.05, the top 20 pathways, including those related to cancer, cytokine-cytokine receptor interaction, NF-κB signaling, and the Hippo signaling pathway, were identified (Figure 1F). The GSEA for the NF-κB signaling pathway is illustrated in Figure 1G. Based on these findings, we focused on the NF-κB signaling pathway to elucidate the potential mechanisms related to t(4;14) MM.

Ivermectin identified as a potential drug using CMap

We used 258 DEGs as potential drug targets for t(4; 14) MM and assessed the CMap database to identify small compounds that could serve as prospective drugs. Table 1 lists the top nine small-molecule drugs believed to hold therapeutic potential in countering the gene expression pattern of t(4;14) MM (with a cut-off score of < −80). Notably, ivermectin, which was listed among the identified small molecules, was considered for further investigation, as it is a high-ranking approved non-chemotherapeutic drug. Thus, we evaluated the potential inhibitory effects of ivermectin on t(4;14) MM cells.

Table 1 Potential drugs identified using the Connectivity Map database

ID	Name	Score	Mechanism of action
BRD-K29733039	Deforolimus	−92.69	mTOR inhibitor
BRD-A48570745	Ivermectin	−91.74	GABA receptor regulator
BRD-K33583600	Isoliquiritigenin	−91.69	Guanylate cyclase activator
BRD-K59456551	Methotrexate	−90.69	Dihydrofolate reductase inhibitor
BRD-A43150328	Penicillic acid	−87.56	Another antibiotic
BRD-A64479082	Quinidine	−85.76	Sodium channel blocker
BRD-K35377380	I-OMe-AG-538	−83.43	IGF-1 inhibitor
BRD-K59570838	Homoveratrylamine	−82.67	Dopamine analog
BRD-A50675702	Fipronil	−80.55	GABA gated chloride channel blocker

mTOR: Mammalian target of rapamycin; GABA: Gamma-aminobutyric acid; IGF-1: Insulin-like growth factor-1.

Molecular docking

Molecular docking is a pivotal technique for the design of structure-based drugs. It facilitates the assessment of molecular interactions by determining the most favorable conformation between small-molecule targets and compounds. The 2D structure of ivermectin is shown in Figure 2A. In molecular docking simulations, ivermectin displayed strong binding affinity to all 10 identified targets, with docking energy scores below −7 kcal/mol (Figure 2B). Notably, CD45 and CYBB demonstrated the most potent binding, with binding energies of −10.2 kcal/mol and −9.9 kcal/mol, respectively. The 3D structural analysis revealedfavorable binding sites for ivermectin in both CD45 (Figure 2E) and CYBB (Figure 2F). Additionally, 2D interaction diagrams indicated hydrogen bond formation between ivermectin and specific amino acid residues in CD45 (Glu1030 and Glu1003) and CYBB (Art73), along with hydrophobic interactions in CD45 (Figure 2C) and water-mediated interactions in CYBB (Figure 2D). These findings shed light on the binding mechanisms underlying the strong affinity between ivermectin and its targets, providing valuable insights for future drug design.

Ivermectin inhibits the proliferation of t(4;14) MM cells

We evaluated the impact of ivermectin on t(4;14) MM cell proliferation by subjecting cells to varying concentrations (0, 4, 6, 8, 10, and 20 μmol/L) of ivermectin and time intervals (24 and 48 h) of exposure. Cell viability, determined using CCK8, demonstrated a significant, concentration- and time-dependent decrease in cancer cell viability (Figure 3A and B). The half-maximum inhibitory concentration (IC_{50}) of ivermectin was approximately 9.4 μmol/L in NCI-H929 cells.

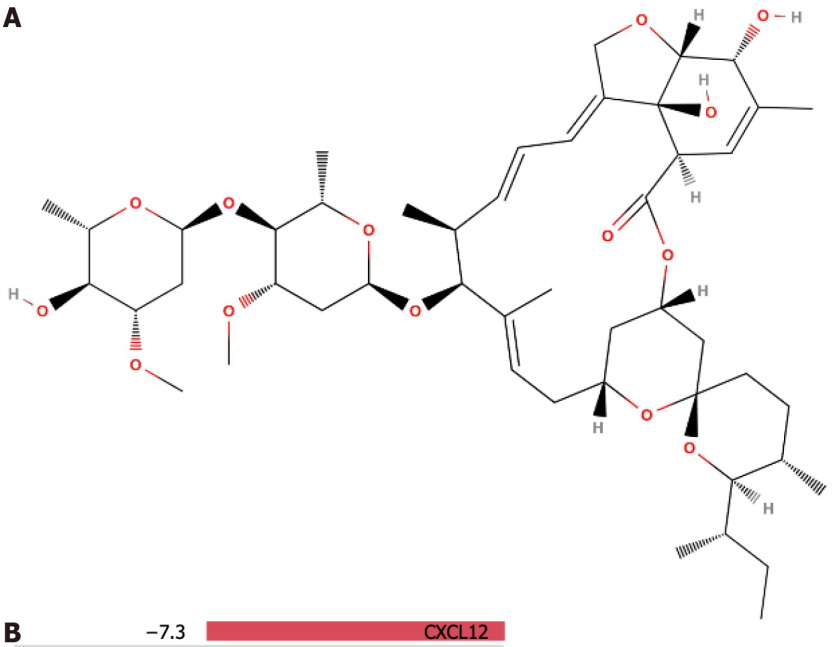
A

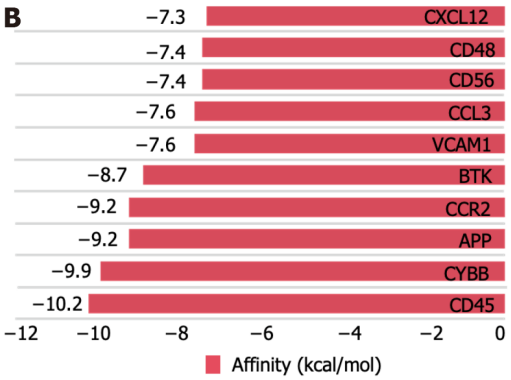
B
−7.3 CXCL12
−7.4 CD48
−7.4 CD56
−7.6 CCL3
−7.6 VCAM1
−8.7 BTK
−9.2 CCR2
−9.2 APP
−9.9 CYBB
−10.2 CD45
−12 −10 −8 −6 −4 −2 0
Affinity (kcal/mol)

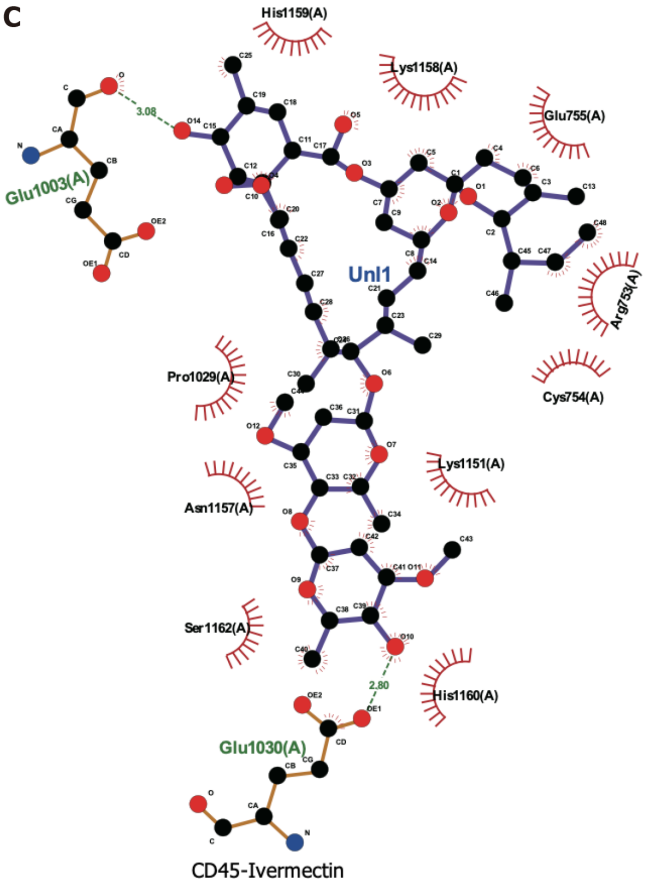
C
His1159(A)
Lys1158(A)
Glu755(A)
Glu1003(A)
Unl1
Arg753(A)
Pro1029(A)
Cys754(A)
Lys1151(A)
Asn1157(A)
Ser1162(A)
His1160(A)
Glu1030(A)
CD45-Ivermectin

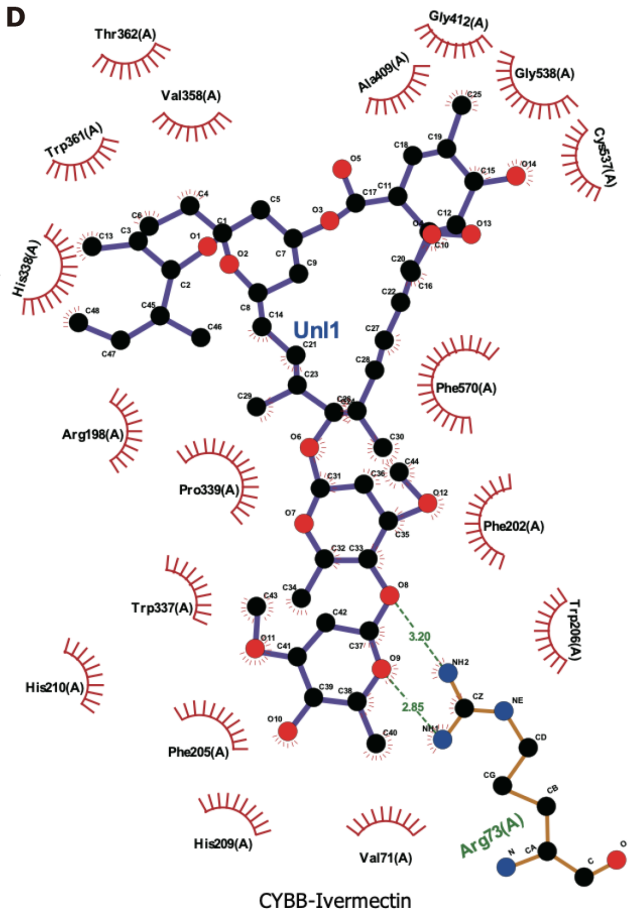
D
Thr362(A)
Gly412(A)
Ala409(A)
Gly538(A)
Val358(A)
Trp361(A)
Cys537(A)
His338(A)
Unl1
Phe570(A)
Arg198(A)
Pro339(A)
Phe202(A)
Trp337(A)
Trp206(A)
His210(A)
Phe205(A)
His209(A)
Val71(A)
Arg73(A)
CYBB-Ivermectin

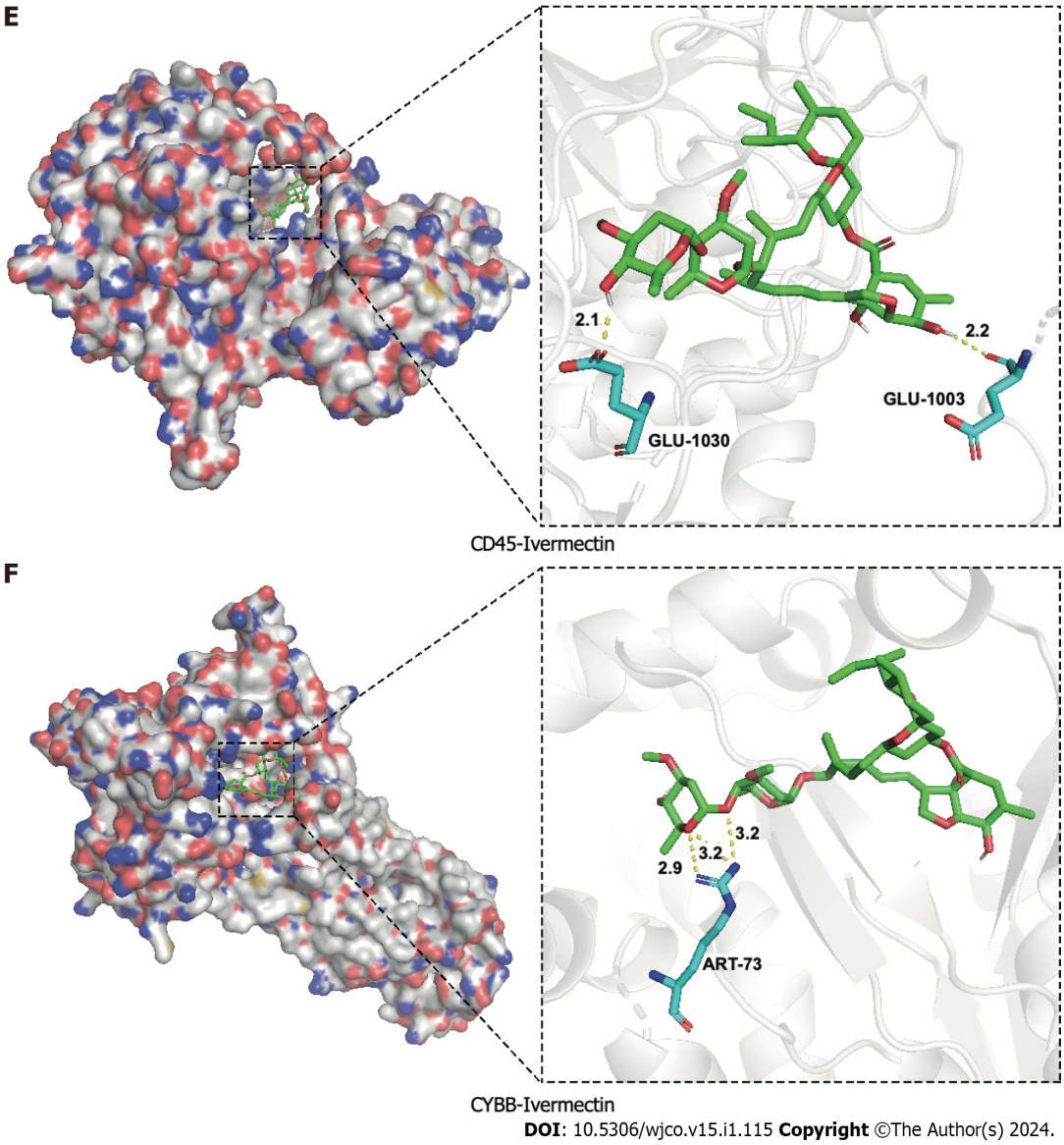

DOI: 10.5306/wjco.v15.i1.115 **Copyright** ©The Author(s) 2024.

Figure 2 Molecular docking analysis of ivermectin with hub target genes. A: Chemical structure of ivermectin; B: Binding affinity of ivermectin with the top 10 hub- target genes. A longer bar indicates a lower binding affinity; C: 2D interaction diagrams of ivermectin with CYBB; D: 2D interaction diagrams of ivermectin with CD45; E: 3D docking structures and interactions of ivermectin with CD45; F: 3D docking structures and interactions of ivermectin with CYBB.

Ivermectin induces apoptosis in t(4;14) MM cells

Drug-induced apoptosis is the primary mechanism underlying cancer cell death[18]. To assess this, we analyzed the expression of the pro- and anti-apoptotic proteins BAX and BCL2, respectively, after treatment and further inspected the BAX/BCL2 ratio. We observed that ivermectin induced apoptosis in t(4;14) MM cells, as evidenced by the upregulation of pro-apoptotic protein BAX and a decrease in anti-apoptotic protein BCL2 levels (Figure 3C). The BAX/BCL2 ratio significantly increased (Figure 3D), and the intrinsic mitochondrial apoptotic pathway was activated, as indicated by elevated caspase-9, caspase-3, downstream effector caspase-3, and PARP expression levels (Figure 3E and F). Annexin V-FITC/propidium iodide staining revealed a substantial increase in the proportion of apoptotic t(4;14) MM cells after ivermectin treatment compared with that of the control (Figure 3G and H), highlighting that the suppressive effect of ivermectin on t(4; 14) MM cells was associated with apoptosis.

Ivermectin increases ROS accumulation and alters the mitochondrial membrane potential in t(4;14) MM cells

Mitochondria are widely known to be the intracellular source of ROS. These species can trigger oxidative damage, leading to a series of mitochondria-related events, including apoptosis[19]. We detected a significant accumulation of ROS in t(4;14) MM cells treated with ivermectin compared with that in untreated controls (Figure 4A). We also observed a notable reduction in the mitochondrial membrane potential (Figure 4B and C), suggesting that ivermectin-induced apoptosis in t(4;14) MM cells was related to mitochondrial function. Collectively, these findings suggest a relationship between ivermectin-induced apoptosis in t(4;14) MM cells and altered mitochondrial dynamics.

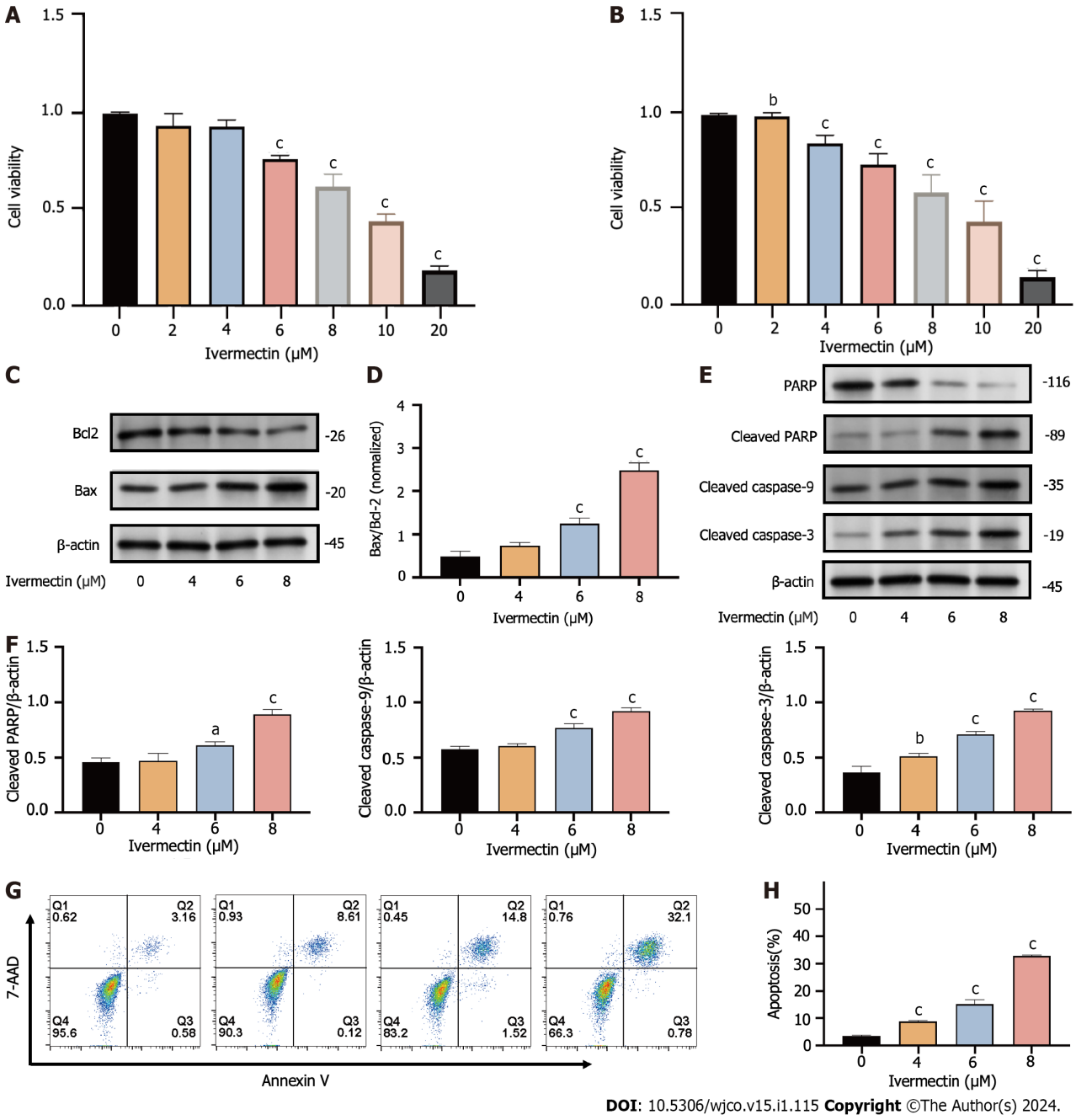

DOI: 10.5306/wjco.v15.i1.115

Figure 3 Ivermectin inhibits proliferation and promotes apoptosis in t(4; 14) multiple myeloma cells. A: CCK-8 analysis of cell viability in cells treated with ivermectin for 24 h; B: CCK-8 analysis of cell viability in cells treated with ivermectin for 48 h; C: Western blot analysis revealing Bax and Bcl-2 protein expression levels in cells treated with ivermectin; D: The relative Bax protein expression levels to Bcl-2 protein expression levels are presented as the means ± SD of three independent experiments; E: Western blot analysis displaying protein expression levels of caspase cascade (including cleaved-caspase 9, cleaved-caspase 3, PARP, and cleaved PARP); F: The data are shown as the means ± SD of three independent experiments. G: Apoptosis in t(4;14) multiple myeloma cells post-ivermectin treatment using 7-AAD/Annexin-V flow cytometry assay. H: The data are shown as the means ± SD of three independent experiments. $^{a}P < 0.05$, $^{b}P < 0.01$, and $^{c}P < 0.001$ compared with the control group.

Ivermectin triggers apoptosis in t(4;14) MM cells via NF-κB signaling pathway

The NF-κB signaling pathway plays a crucial role in the onset and progression of the disease in t(4;14) MM, often exhibiting overactivation in these cells and promoting their survival[20]. Our results revealed that ivermectin treatment substantially reduced both the protein expression and phosphorylation levels of NF-κB p65 in a dose-dependent manner (Figure 4D and E). Furthermore, the protein expression and phosphorylation levels of IκBα, a regulator upstream of NF-κB, were also suppressed in t(4;14) MM cells post-ivermectin treatment.

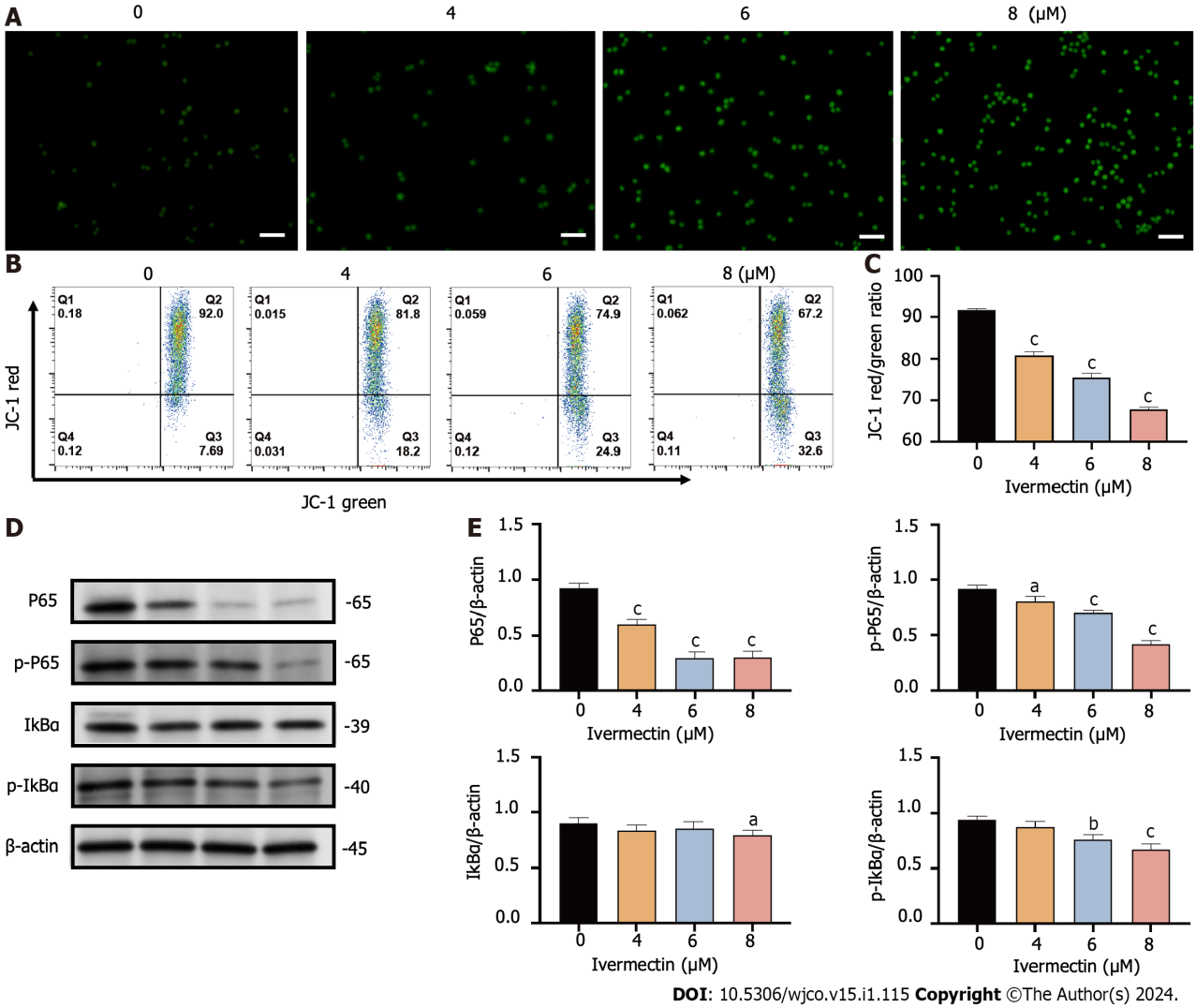

DOI: 10.5306/wjco.v15.i1.115

Figure 4 Ivermectin induces apoptosis in t(4;14) multiple myeloma cells *via* mitochondrial and nuclear factor-κB signaling pathway. A: Visualization of intracellular reactive oxygen species (ROS) in t(4;14) multiple myeloma (MM) cells after treatment with ivermectin using 2',7'-dichlorodihydrofluorescein (DCF) diacetate staining. ROS is represented by the green DCF fluorescence viewed under a fluorescence microscope at 200× magnification. Scale bar: 50 μm. B: Mitochondrial membrane potential in t(4;14) MM cells post-ivermectin treatment assessed using JC-1 staining; C: The data are shown as the means ± SD of three independent experiments; D: Expression patterns of p65, p-p65, p-IκBα, and IκBα in t(4;14) MM cells after exposure to ivermectin, analyzed by western blotting; E: The data are shown as the means ± SD of three independent experiments. $^{a}P < 0.05$, $^{b}P < 0.01$, and $^{c}P < 0.001$ compared with the control group.

DISCUSSION

MM is a multifaceted and incurable disease that displays vast heterogeneity in its clinical manifestations, genetic changes, therapeutic responses, and overall prognosis[2]. Guidelines from bodies, such as the International Myeloma Working Group, recognize t(4;14) MM as a high-risk cytogenetic abnormality[21]. The t(4;14) MM subtype continues to present a challenging prognosis despite advances in drug therapies[22]. Therefore, there is an urgent need to develop new therapeutic drugs to treat t(4;14) MM. Recent studies have highlighted the potential of identifying molecular targets and therapeutic drugs for MM through expression profiling and functional enrichment analyses. Di Meo *et al*[23] identified ILT3 as an immunotherapeutic target for MM, whereas Mereu *et al*[24] revealed that UNC0642 increasedcarfilzomib sensitivity and counteracted drug resistance in MM cell lines. In this study, we identified the key genes and prospective therapeutic agents for t(4;14) MM using gene expression profile analysis.

The regulation of the immune response is fundamental for the development and progression of MM[25]. We identified CD45, CD48, and CD56 as the key genes in t(4;14) MM. Compared with healthy bone marrow controls, patients with t(4;14) MM exhibited decreased CD45 expression levels, whereas CD48 and CD56 levels were notably increased. CD45, also known as protein tyrosine phosphatase receptor type C, was previously called the common leukocyte antigen. This protein is essential for modulating antigen receptor signaling, which is crucial for lymphocyte development, survival, and function[26]. However, the role of CD45 in MM remains elusive. Evidence suggests thatCD45 expression decreases during MM progression[27]. As mature MM cells are predominantly CD45-negative and have inactive SRC family kinases, they remain unaffected by elotuzumab[28]. Moreover, MM cells in high-risk genetic categories tend to express

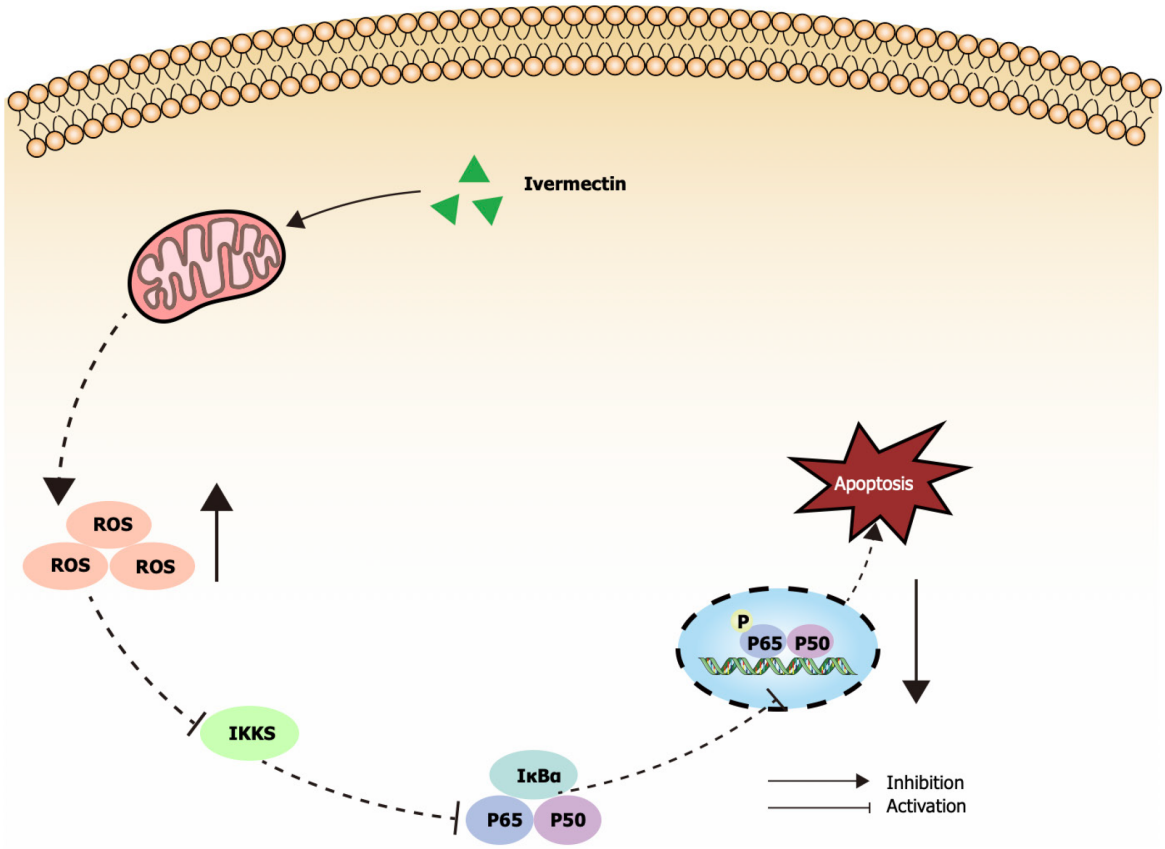

DOI: 10.5306/wjco.v15.i1.115 **Copyright** ©The Author(s) 2024.

Figure 5 Illustrated overview of ivermectin promoting apoptosis in t(4;14) multiple myeloma cells. IκBα: Anti-inhibitor of NF-κB; IKKs: Inhibitors of kappa B kinase; ROS: Reactive oxygen species.

reduced CD45 levels[29]. CD48[30], a member of the signaling lymphocytic activation molecule family, plays a role in immune cell adhesion and activation. Although it is present in almost all MM plasma cells, it is absent from non-hematopoietic tissues. Van Acker *et al*[31] identified CD48 as a promising molecular target for the therapy of MM antibody therapy. CD56, a neural cell adhesion molecule, is a glycoprotein present in neural and muscle tissues, as well as in myeloma cells. Cottini *et al*[32] observed its high expression levels in the t(4;14) MM cell line NCI-H929. CD56 boosts MM cell growth and influences adhesion to stromal cells. Collectively, these findings highlight the potential for a deeper evaluation of immune phenotypes for both diagnosis and treatment of t(4;14) MM.

In this study, we also utilized the CMap database to identify potential small-molecule drugs targeting t(4;14) MM. Our primary focus was on molecular docking and subsequent experimental validation of the predicted drug, ivermectin. Traditionally, ivermectin is a macrocyclic lactone antibiotic used to treat parasitic diseases[33]. Recent studies have revealed its potential antitumor capabilities in various cancers, including breast[34] and pancreatic[35] cancer. Emerging evidence also suggests its synergistic lethal effects on MM cells when combined with proteasome inhibitors[36]. However, a comprehensive understanding of the specific action mechanisms of ivermectin against MM, especially the t(4;14) subtype, remains elusive. Our findings demonstrate that ivermectin suppresses the growth of t(4;14) MM cells, as well as triggers apoptosis.

The NF-κB signaling pathway is crucial for driving cancer progression, angiogenesis, and shaping the tumor microenvironment[37]. It orchestrates the production of pro-inflammatory cytokines, inflammatory mediators, and cell adhesion molecules, creating a favorable microenvironment for MM initiation and progression[38]. Consequently, many leading anti-MM drugs indirectly target the NF-κB signaling pathway[39]. Bortezomib hinders the proteasomal degradation of NF-κB and IκB proteins, inhibiting gene transcription activation[40]. Our findings revealed a pronounced suppression of the NF-κB signaling pathway in ivermectin-treated t(4;14) MM cells (Figure 5). This suggests that ivermectin, by acting as an external signaling agent, inhibits the activation of this pathway, reducing anti-apoptotic effects and thereby enhancing cell apoptosis.

Mitochondria are essential for cell survival, functioning as the primary source of ROS and producing adenosine triphosphate (ATP) through oxidative phosphorylation[41]. In a pathological state, mitochondrial dysfunction results inATP depletion[42]. In the current study, treatment of t(4;14) MM with ivermectin led to elevated ROS levels and decreased cell membrane potential. These findings, along with previous reports, suggest that ivermectin exposure can induce oxidative stress and disrupt the mitochondrial balance, facilitating the apoptosis of t(4;14) MM cells.

There are also some limitations of the present study. Firstly, the sample size may be insufficient, potentially leading to selection bias. Secondly, regarding the experiments on ivermectin against t(4;14) MM, this study has only completed a portion of the *in vitro* experiments, and further validation of its effectiveness and safety is still required in *in vivo*

experiments. Furthermore, additional genetic and experimental studies are needed to elucidate the mechanisms and functions of these key genes in the occurrence and development of t(4;14) translocated multiple myeloma.

CONCLUSION

In conclusion, we utilized bioinformatics tools, molecular docking, and experimental validation to identify key genes and potential treatments for t(4;14) MM. Notably, we confirmed that ivermectin induced apoptosis in t(4;14) MM cells *via* the NF-κB signaling pathway. However, these insights require additional exploration and robust validation in further studies.

ARTICLE HIGHLIGHTS

Research background

Multiple myeloma (MM) is a terminally differentiated B-cell tumor disease with a challenging prognosis. Specifically, the t(4;14) MM is categorized as a high-risk subtype within MM.

Research motivation

The t(4;14) MM tends to relapse, and currently, there is a lack of effective clinical treatment strategies.

Research objectives

This study aimed to elucidate the molecular basis of the t(4;14) MM and search for potential effective drugs through a comprehensive approach.

Research methods

The transcriptional characteristics of t(4;14) multiple myeloma were obtained from the Gene Expression Omnibus and subjected to gene ontology and pathway enrichment analysis. Utilizing the STRING database and Cytoscape, a protein-protein interaction network was constructed, and core targets were identified. Connectivity Map identified potential small-molecule drugs, and these findings were validated through molecular docking analysis. One of these drugs, ivermectin, was further tested for its effects on t(4;14) multiple myeloma cells.

Research results

We identified 258 differentially expressed genes with enriched functions in cancer pathways, cytokine receptor interactions, the nuclear factor (NF)-kappa B signaling pathway. Ten key genes were pinpointed. Ivermectin emerged as a potential treatment. *In vitro*, ivermectin inhibited t(4;14) MM cell growth *via* the NF-kappa B pathway and induced t(4;14) MM cell apoptosis.

Research conclusions

Ivermectin induced apoptosis in t(4;14) MM cells *via* the NF-κB signaling pathway.

Research perspectives

Our study offers valuable molecular insights for biomarker validation and potential drug development in t(4;14) MM diagnosis and treatment.

FOOTNOTES

Author contributions: Song Y and Lu XC conceived and designed the experiments. Zhang HJ, Geng J, and Song Y conducted the experiments and drafted the manuscript; Zhong LZ and Song X contributed to the techniques used and commented on the manuscript; Li HY performed the data analysis; Yang B and Lu XC assisted with revising the manuscript; All the authors reviewed the results and approved the final version of the manuscript.

Supported by the National Key Research and Development Program of China, No. 2021YFC2701704; the National Clinical Medical Research Center for Geriatric Diseases, "Multicenter RCT" Research Project, No. NCRCG-PLAGH-20230010; and the Military Logistics Independent Research Project, No. 2022HQZZ06.

Institutional review board statement: This study does not involve research on humans/animals and does not include the initial version formally approved by the Institutional Review Board in the official language of the authors' country.

Informed consent statement: This study does not involve clinical research and does not include the initial version of the informed consent form signed by all subjects and investigators.

Conflict-of-interest statement: The authors declare that they have no known competing financial interests or personal relationships that could have appeared to influence the work reported in this paper.

Data sharing statement: No additional data are available.

Country/Territory of origin: China

ORCID number: Xue-Chun Lu 0000-0002-8937-2278.

S-Editor: Liu JH
L-Editor: A
P-Editor: Zhang XD

REFERENCES

1 **Siegel RL**, Miller KD, Wagle NS, Jemal A. Cancer statistics, 2023. *CA Cancer J Clin* 2023; **73**: 17-48 [PMID: 36633525 DOI: 10.3322/caac.21763]
2 **Cowan AJ**, Green DJ, Kwok M, Lee S, Coffey DG, Holmberg LA, Tuazon S, Gopal AK, Libby EN. Diagnosis and Management of Multiple Myeloma: A Review. *JAMA* 2022; **327**: 464-477 [PMID: 35103762 DOI: 10.1001/jama.2022.0003]
3 **Abdallah N**, Rajkumar SV, Greipp P, Kapoor P, Gertz MA, Dispenzieri A, Baughn LB, Lacy MQ, Hayman SR, Buadi FK, Dingli D, Go RS, Hwa YL, Fonder A, Hobbs M, Lin Y, Leung N, Kourelis T, Warsame R, Siddiqui M, Lust J, Kyle RA, Bergsagel L, Ketterling R, Kumar SK. Cytogenetic abnormalities in multiple myeloma: association with disease characteristics and treatment response. *Blood Cancer J* 2020; **10**: 82 [PMID: 32782240 DOI: 10.1038/s41408-020-00348-5]
4 **Foltz SM**, Gao Q, Yoon CJ, Sun H, Yao L, Li Y, Jayasinghe RG, Cao S, King J, Kohnen DR, Fiala MA, Ding L, Vij R. Evolution and structure of clinically relevant gene fusions in multiple myeloma. *Nat Commun* 2020; **11**: 2666 [PMID: 32471990 DOI: 10.1038/s41467-020-16434-y]
5 **Ashby C**, Boyle EM, Bauer MA, Mikulasova A, Wardell CP, Williams L, Siegel A, Blaney P, Braunstein M, Kaminetsky D, Keats J, Maura F, Landgren O, Walker BA, Davies FE, Morgan GJ. Structural variants shape the genomic landscape and clinical outcome of multiple myeloma. *Blood Cancer J* 2022; **12**: 85 [PMID: 35637217 DOI: 10.1038/s41408-022-00673-x]
6 **Zhang Z**, Zhou L, Xie N, Nice EC, Zhang T, Cui Y, Huang C. Overcoming cancer therapeutic bottleneck by drug repurposing. *Signal Transduct Target Ther* 2020; **5**: 113 [PMID: 32616710 DOI: 10.1038/s41392-020-00213-8]
7 **Hernández-Lemus E**, Martínez-García M. Pathway-Based Drug-Repurposing Schemes in Cancer: The Role of Translational Bioinformatics. *Front Oncol* 2020; **10**: 605680 [PMID: 33520715 DOI: 10.3389/fonc.2020.605680]
8 **Martin KH**, Slack JK, Boerner SA, Martin CC, Parsons JT. Integrin connections map: to infinity and beyond. *Science* 2002; **296**: 1652-1653 [PMID: 12040184 DOI: 10.1126/science.296.5573.1652]
9 **Shi X**, Zhang W, Bao X, Liu X, Yang M, Yin C. Eugenol modulates the NOD1-NF-κB signaling pathway *via* targeting NF-κB protein in triple-negative breast cancer cells. *Front Endocrinol (Lausanne)* 2023; **14**: 1136067 [PMID: 36923216 DOI: 10.3389/fendo.2023.1136067]
10 **Qiu HZ**, Huang J, Xiang CC, Li R, Zuo ED, Zhang Y, Shan L, Cheng X. Screening and Discovery of New Potential Biomarkers and Small Molecule Drugs for Cervical Cancer: A Bioinformatics Analysis. *Technol Cancer Res Treat* 2020; **19**: 1533033820980112 [PMID: 33302814 DOI: 10.1177/1533033820980112]
11 **Szklarczyk D**, Gable AL, Lyon D, Junge A, Wyder S, Huerta-Cepas J, Simonovic M, Doncheva NT, Morris JH, Bork P, Jensen LJ, Mering CV. STRING v11: protein-protein association networks with increased coverage, supporting functional discovery in genome-wide experimental datasets. *Nucleic Acids Res* 2019; **47**: D607-D613 [PMID: 30476243 DOI: 10.1093/nar/gky1131]
12 **Chin CH**, Chen SH, Wu HH, Ho CW, Ko MT, Lin CY. cytoHubba: identifying hub objects and sub-networks from complex interactome. *BMC Syst Biol* 2014; **8** Suppl 4: S11 [PMID: 25521941 DOI: 10.1186/1752-0509-8-S4-S11]
13 **Yang K**, Dinasarapu AR, Reis ES, Deangelis RA, Ricklin D, Subramaniam S, Lambris JD. CMAP: Complement Map Database. *Bioinformatics* 2013; **29**: 1832-1833 [PMID: 23661693 DOI: 10.1093/bioinformatics/btt269]
14 **UniProt Consortium**. UniProt: a hub for protein information. *Nucleic Acids Res* 2015; **43**: D204-D212 [PMID: 25348405 DOI: 10.1093/nar/gku989]
15 **Kim S**, Chen J, Cheng T, Gindulyte A, He J, He S, Li Q, Shoemaker BA, Thiessen PA, Yu B, Zaslavsky L, Zhang J, Bolton EE. PubChem 2019 update: improved access to chemical data. *Nucleic Acids Res* 2019; **47**: D1102-D1109 [PMID: 30371825 DOI: 10.1093/nar/gky1033]
16 **Laskowski RA**, Swindells MB. LigPlot+: multiple ligand-protein interaction diagrams for drug discovery. *J Chem Inf Model* 2011; **51**: 2778-2786 [PMID: 21919503 DOI: 10.1021/ci200227u]
17 **Delano WL**. Pymol: an open-source molecular graphics tool. *CCP4 Newsl Protein Crystallogr* 2002; **40**: 82-92 [DOI: 10.1101/2020.06.16.154773]
18 **Singh P**, Lim B. Targeting Apoptosis in Cancer. *Curr Oncol Rep* 2022; **24**: 273-284 [PMID: 35113355 DOI: 10.1007/s11912-022-01199-y]
19 **Nakamura H**, Takada K. Reactive oxygen species in cancer: Current findings and future directions. *Cancer Sci* 2021; **112**: 3945-3952 [PMID: 34286881 DOI: 10.1111/cas.15068]
20 **Yu H**, Lin L, Zhang Z, Zhang H, Hu H. Targeting NF-κB pathway for the therapy of diseases: mechanism and clinical study. *Signal Transduct Target Ther* 2020; **5**: 209 [PMID: 32958760 DOI: 10.1038/s41392-020-00312-6]

21 **Hagen P**, Zhang J, Barton K. High-risk disease in newly diagnosed multiple myeloma: beyond the R-ISS and IMWG definitions. *Blood Cancer J* 2022; **12**: 83 [PMID: 35637223 DOI: 10.1038/s41408-022-00679-5]

22 **Sonneveld P**, Avet-Loiseau H, Lonial S, Usmani S, Siegel D, Anderson KC, Chng WJ, Moreau P, Attal M, Kyle RA, Caers J, Hillengass J, San Miguel J, van de Donk NW, Einsele H, Bladé J, Durie BG, Goldschmidt H, Mateos MV, Palumbo A, Orlowski R. Treatment of multiple myeloma with high-risk cytogenetics: a consensus of the International Myeloma Working Group. *Blood* 2016; **127**: 2955-2962 [PMID: 27002115 DOI: 10.1182/blood-2016-01-631200]

23 **Di Meo F**, Iyer A, Akama K, Cheng R, Yu C, Cesarano A, Kurihara N, Tenshin H, Aljoufi A, Marino S, Soni RK, Roda J, Sissons J, Vu LP, Guzman M, Huang K, Laskowski T, Broxmeyer HE, Roodman DG, Perna F. A target discovery pipeline identified ILT3 as a target for immunotherapy of multiple myeloma. *Cell Rep Med* 2023; **4**: 101110 [PMID: 37467717 DOI: 10.1016/j.xcrm.2023.101110]

24 **Mereu E**, Abbo D, Paradzik T, Cumerlato M, Bandini C, Labrador M, Maccagno M, Ronchetti D, Manicardi V, Neri A, Piva R. Euchromatic Histone Lysine Methyltransferase 2 Inhibition Enhances Carfilzomib Sensitivity and Overcomes Drug Resistance in Multiple Myeloma Cell Lines. *Cancers (Basel)* 2023; **15** [PMID: 37190128 DOI: 10.3390/cancers15082199]

25 **Swamydas M**, Murphy EV, Ignatz-Hoover JJ, Malek E, Driscoll JJ. Deciphering mechanisms of immune escape to inform immunotherapeutic strategies in multiple myeloma. *J Hematol Oncol* 2022; **15**: 17 [PMID: 35172851 DOI: 10.1186/s13045-022-01234-2]

26 **Al Barashdi MA**, Ali A, McMullin MF, Mills K. Protein tyrosine phosphatase receptor type C (PTPRC or CD45). *J Clin Pathol* 2021; **74**: 548-552 [PMID: 34039664 DOI: 10.1136/jclinpath-2020-206927]

27 **Robillard N**, Pellat-Deceunynck C, Bataille R. Phenotypic characterization of the human myeloma cell growth fraction. *Blood* 2005; **105**: 4845-4848 [PMID: 15741217 DOI: 10.1182/blood-2004-12-4700]

28 **Guo H**, Cruz-Munoz ME, Wu N, Robbins M, Veillette A. Immune cell inhibition by SLAMF7 is mediated by a mechanism requiring src kinases, CD45, and SHIP-1 that is defective in multiple myeloma cells. *Mol Cell Biol* 2015; **35**: 41-51 [PMID: 25312647 DOI: 10.1128/MCB.01107-14]

29 **Radzevičius M**, Dirsė V, Klimienė I, Matuzevičienė R, Kučinskienė ZA, Pečeliūnas V. Multiple Myeloma Immunophenotype Related to Chromosomal Abnormalities Used in Risk Assessment. *Diagnostics (Basel)* 2022; **12** [PMID: 36140450 DOI: 10.3390/diagnostics12092049]

30 **McArdel SL**, Terhorst C, Sharpe AH. Roles of CD48 in regulating immunity and tolerance. *Clin Immunol* 2016; **164**: 10-20 [PMID: 26794910 DOI: 10.1016/j.clim.2016.01.008]

31 **Van Acker HH**, Capsomidis A, Smits EL, Van Tendeloo VF. CD56 in the Immune System: More Than a Marker for Cytotoxicity? *Front Immunol* 2017; **8**: 892 [PMID: 28791027 DOI: 10.3389/fimmu.2017.00892]

32 **Cottini F**, Rodriguez J, Hughes T, Sharma N, Guo L, Lozanski G, Liu B, Cocucci E, Yang Y, Benson D. Redefining CD56 as a Biomarker and Therapeutic Target in Multiple Myeloma. *Mol Cancer Res* 2022; **20**: 1083-1095 [PMID: 35380709 DOI: 10.1158/1541-7786.MCR-21-0828]

33 **Laing R**, Gillan V, Devaney E. Ivermectin - Old Drug, New Tricks? *Trends Parasitol* 2017; **33**: 463-472 [PMID: 28285851 DOI: 10.1016/j.pt.2017.02.004]

34 **Draganov D**, Han Z, Rana A, Bennett N, Irvine DJ, Lee PP. Ivermectin converts cold tumors hot and synergizes with immune checkpoint blockade for treatment of breast cancer. *NPJ Breast Cancer* 2021; **7**: 22 [PMID: 33654071 DOI: 10.1038/s41523-021-00229-5]

35 **Lee DE**, Kang HW, Kim SY, Kim MJ, Jeong JW, Hong WC, Fang S, Kim HS, Lee YS, Kim HJ, Park JS. Ivermectin and gemcitabine combination treatment induces apoptosis of pancreatic cancer cells *via* mitochondrial dysfunction. *Front Pharmacol* 2022; **13**: 934746 [PMID: 36091811 DOI: 10.3389/fphar.2022.934746]

36 **Luo H**, Feng Y, Wang F, Lin Z, Huang J, Li Q, Wang X, Liu X, Zhai X, Gao Q, Li L, Zhang Y, Wen J, Zhang L, Niu T, Zheng Y. Combinations of ivermectin with proteasome inhibitors induce synergistic lethality in multiple myeloma. *Cancer Lett* 2023; **565**: 216218 [PMID: 37149018 DOI: 10.1016/j.canlet.2023.216218]

37 **Napetschnig J**, Wu H. Molecular basis of NF-κB signaling. *Annu Rev Biophys* 2013; **42**: 443-468 [PMID: 23495970 DOI: 10.1146/annurev-biophys-083012-130338]

38 **Wong AH**, Shin EM, Tergaonkar V, Chng WJ. Targeting NF-κB Signaling for Multiple Myeloma. *Cancers (Basel)* 2020; **12** [PMID: 32781681 DOI: 10.3390/cancers12082203]

39 **Vrábel D**, Pour L, Ševčíková S. The impact of NF-κB signaling on pathogenesis and current treatment strategies in multiple myeloma. *Blood Rev* 2019; **34**: 56-66 [PMID: 30501907 DOI: 10.1016/j.blre.2018.11.003]

40 **Paramore A**, Frantz S. Bortezomib. *Nat Rev Drug Discov* 2003; **2**: 611-612 [PMID: 12908468 DOI: 10.1038/nrd1159]

41 **Zhang B**, Pan C, Feng C, Yan C, Yu Y, Chen Z, Guo C, Wang X. Role of mitochondrial reactive oxygen species in homeostasis regulation. *Redox Rep* 2022; **27**: 45-52 [PMID: 35213291 DOI: 10.1080/13510002.2022.2046423]

42 **Ma Z**, Han H, Zhao Y. Mitochondrial dysfunction-targeted nanosystems for precise tumor therapeutics. *Biomaterials* 2023; **293**: 121947 [PMID: 36512861 DOI: 10.1016/j.biomaterials.2022.121947]

Published by **Baishideng Publishing Group Inc**
7041 Koll Center Parkway, Suite 160, Pleasanton, CA 94566, USA
Telephone: +1-925-3991568
E-mail: office@baishideng.com
Help Desk: https://www.f6publishing.com/helpdesk
https://www.wjgnet.com